Accepted Manuscript

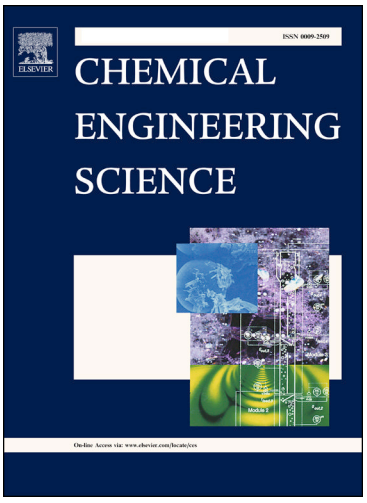

On THE PrediCtions for diffusion-Driven EVAPORATION of sessile droplets With interface cooling

Ha V. Tran, Tuan A.H. Nguyen, Simon R. Biggs, Anh V. Nguyen

PII: S0009-2509(17)30740-6
DOI: https://doi.org/10.1016/j.ces.2017.12.003
Reference: CES 13938

To appear in: *Chemical Engineering Science*

Received Date: 30 August 2017
Revised Date: 14 November 2017
Accepted Date: 3 December 2017

Please cite this article as: H.V. Tran, T.A.H. Nguyen, S.R. Biggs, A.V. Nguyen, On THE PrediCtions for diffusion-Driven EVAPORATION of sessile droplets With interface cooling, *Chemical Engineering Science* (2017), doi: https://doi.org/10.1016/j.ces.2017.12.003

ON THE PREDICTIONS FOR DIFFUSION-DRIVEN EVAPORATION OF SESSILE DROPLETS WITH INTERFACE COOLING

Ha V. Tran, Tuan A. H. Nguyen*, Simon R. Biggs, Anh V. Nguyen*

School of Chemical Engineering, The University of Queensland, Queensland 4072, Australia.

Fax: +61 7 33654199; Email: anh.nguyen@eng.uq.edu.au and tuan.a.h.nguyen@uq.edu.au

ABSTRACT

The diffusion-driven evaporation of sessile droplets from planar surfaces is influenced by cooling at the air-liquid interface. Here, corrections to the available models for predicting the evaporation process are presented. The mass conservation for diffusion-driven evaporation is resolved by considering the effect of interface cooling on the change in density of saturated vapour along the liquid-vapour interface of sessile droplets. Corrections to the predictions for the spatial distribution of vapour density around a sessile droplet and the evaporative flux of vapour at the interface are obtained. The classical models are recovered from the new predictions if interface cooling is negligible. Comparison between the new and classical predictions for the local surface evaporative flux is obtained using the literature data. Our analysis shows a significant effect of interface cooling which should be considered in predicting diffusion-driven evaporation of sessile droplets on planar surfaces.

Keywords: coffee ring, contact angle, flux, toroidal coordinate, Laplace equation.

1. Introduction

Diffusion-driven evaporation of sessile droplets on planar surfaces plays an important role in a number of industrial applications such as the supply of foliar fertilizers, pesticides, and insecticides to plants through the leaf surface, drying of dairy product, spray cooling, ink-jet printing, and coating. Research over the last two decades has focused on understanding how the contact angle and contact line at the intersection between the droplet surface and the solid surface influence the evaporation kinetics. Droplet evaporation has been explained and described by applying a number of modes (Nguyen and Nguyen, 2012a; Picknett and Bexon, 1977), including the constant-contact-angle, constant-contact-radius, and stick-slip modes.

The underlying theory is based on mass conservation for the vapour evaporation by diffusion, as described by Fick's second law. For example, researchers (Deegan et al., 1997; Erbil, 2015; Picknett and Bexon, 1977) have applied the theory to explain the coffee-ring effect on evaporation

of suspensions of colloidal particles. The key equation for a non-uniform local evaporative flux, $J(\alpha)$, was obtained as a function of contact angle, θ, between the gas-liquid and solid-liquid interfaces as follows:

$$J_{classic} = \frac{C_s - C_\infty}{R/D}\left\{\frac{\sin\theta}{2} + \sqrt{2}\left(\cosh\alpha + \cos\theta\right)^{3/2}\int_0^\infty \frac{\tau\cosh\tau\theta}{\cosh\tau\pi}\tanh\left[\tau\left(\pi-\theta\right)\right]P_{i\tau-1/2}\left(\cosh\alpha\right)\,d\tau\right\} \quad [1]$$

where C_s is the constant (saturated) vapour density at the droplet surface, C_∞ is the liquid vapour density far away from the droplet surface (at infinity), R is the droplet base radius, D is the vapour diffusion coefficient, τ is the integration dummy. α is the local position of the droplet surface in the toroidal coordinate system, which is related with its radial coordinate (measured perpendicular to the droplet axis of rotational symmetry) by $r = R\sinh\alpha/\left(\cosh\alpha+\cos\beta\right)$. $P_{i\tau-1/2}\left(\cosh\alpha\right)$ is the toroidal (or ring) function (i.e., the first-kind Legendre function of the complex half-integral degree and the argument of the hyperbolic cosine function) (Magnus et al., 1966) and $i=\sqrt{-1}$ is the imaginary unit.

Equation [1] is very well known in the literature and can be found in many papers, e.g.,(Hu and Larson, 2002; Nguyen and Nguyen, 2012b; Nguyen et al., 2012; Popov, 2005). It presents one of the key classical models of diffusion-driven evaporation of sessile droplets on a planar surface and has provided the framework for further investigations. Recently, the models have been extended to describe the diffusion-driven evaporation of sessile droplets affected by interface cooling. In this extension, the constant vapour density at the droplet surface, such as C_s in Eq. [1], is replaced by a function of the local surface coordinate, $C_s(\alpha)$, yielding (Gleason and Putnam, 2014)

$$J_{GP} = \frac{C_s(\alpha) - C_\infty}{R/D}\left\{\frac{\sin\theta}{2} + \sqrt{2}\left(\cosh\alpha + \cos\theta\right)^{3/2}\int_0^\infty \frac{\tau\cosh\tau\theta}{\cosh\tau\pi}\tanh\left[\tau\left(\pi-\theta\right)\right]P_{i\tau-1/2}\left(\cosh\alpha\right)\,d\tau\right\} \quad [2]$$

Function, $C_s(\alpha)$, of vapour saturation density at the droplet surface in Eq. [2] was determined by interpolating the experimental results for the droplet surface temperature (Gleason and Putnam, 2014).

In this paper, the effect of interface cooling on diffusion-driven evaporation of sessile droplets is re-examined. The new corrections to the available models for diffusion-driven evaporation of sessile droplets are established. We show that the newly established models for

describing the diffusion-driven evaporation of sessile droplets affected by interface cooling, such as that described by Eq. [2], have to be corrected.

2. Theoretical analysis

We consider a sessile droplet of the spherical-cap shape placed on a solid planar surface. The sessile droplet has rotational symmetry about the direction of gravity. It can suitably be described using the cylindrical coordinate system (r, z, φ), whose cylindrical axis (z) is opposite to the direction of gravity (Nguyen et al., 2012). The coordinate system has its origin at the centre of the droplet base and its polar axis (r) lying on the solid surface (Figure 1). Mass conservation of vapour evaporation by diffusion is described by Fick's second law. Specifically, the evaporation is usually described by the well-known Laplace partial differential equation, $\nabla^2 C = 0$, for the liquid vapour density, C, in the half-space above the droplet surface and the planar surface. The Laplace equation can suitably be solved by applying the method of separation of variables in the toroidal coordinate system (α, β, φ) (Nguyen et al., 2012). The solution can be expressed in terms of the normalised vapour concentration, C, as follows:

$$C \equiv \frac{C(\alpha,\beta)-C_\infty}{C_e-C_\infty} = \sqrt{2\cosh\alpha - 2\cos\beta}\int_0^\infty E_\tau P_{i\tau-1/2}(\cosh\alpha)\cosh\left[\tau(2\pi-\beta)\right]d\tau \qquad [3]$$

where $C_e = C_s(\infty)$ is the vapour density at the droplet edge ($\alpha \to \infty$). In Eq. [3], E_τ is a function of the integration dummy (independent of the toroidal coordinates α and β), which can be determined from the boundary conditions. The other symbols are previously defined in conjunction with Eq. [1]. The solution is independent of φ because of the rotational symmetry. The two coordinate systems are linked by a complex mapping, where $z + ir = iR\coth\frac{\alpha+i\beta}{2}$, where R is the base radius of the droplet. The solution is also bounded by the physical domain: $\infty > \alpha \geq 0$ and $3\pi - \theta \geq \beta \geq 2\pi$ as shown in Figure 1.

Since the complex mapping gives $r = \frac{R\sinh\alpha}{\cosh\alpha+\cos\beta}$ and $z = \frac{R\sin\beta}{\cosh\alpha+\cos\beta}$, we have $\sqrt{r^2+z^2} = R\sqrt{\frac{\cosh\alpha+\cos\beta}{\cosh\alpha-\cos\beta}}$, which shows that a point at infinity (i.e., $\sqrt{r^2+z^2} \to \infty$) is characterised by the "point" of $\alpha = 0$ and $\beta = 2\pi$. The other important details for applying the boundary conditions include the following special values of the toroidal coordinates:

1) The droplet edge (i.e., $r = R$ and $z = 0$): $\alpha \to \infty$ and $\beta = 2\pi$,

2) The droplet surface: $\infty > \alpha \geq 0$ and $\beta = 3\pi - \theta$, and

3) The solid surface in the vapour phase: $\infty > \alpha > 0$ and $\beta = 2\pi$.

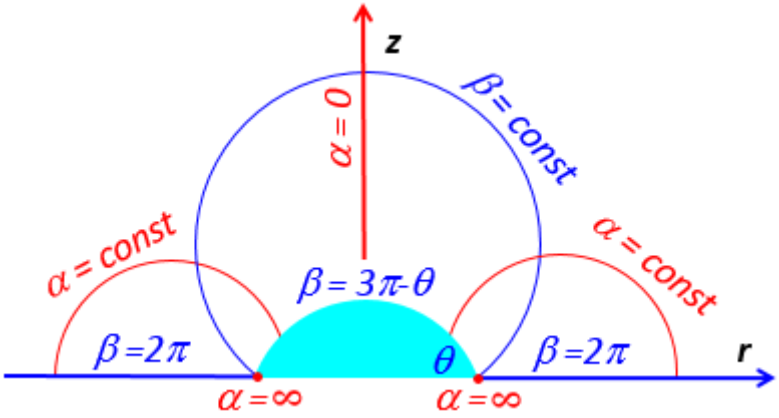

Figure 1. Schematic of the cylindrical co-ordinates (r, z, φ) and the reduced toroidal coordinates (α, β, φ) in the meridian plane (φ = const) used to describe the evaporation of a sessile droplet with a spherical cap shape on a flat surface. The contact angle θ is defined through the liquid phase.

It now can be seen that the solution described by Eq. [3] can identically satisfy the following conditions:

1) The boundary condition at infinity, i.e., $C(0, 2\pi) = C_\infty$ since the term under the square root on the right-hand side of Eq. [3] is equal to 0 when $\alpha \to \infty$ and $\beta = 2\pi$,

2) The symmetric condition at the axis of symmetry: $(\partial C / \partial \alpha)_{a=0} = 0$, and

3) The boundary condition at the solid-vapour interface: $(\partial C / \partial \beta)_{\beta=2\pi} = 0$ for the zero flux of vapour diffusion.

The physical description of the effect of interface cooling during droplet evaporation can be implemented via the boundary condition applied at the droplet surface, i.e., $\beta = 3\pi - \theta$. Traditionally, the vapour concentration at the droplet is considered as a constant as discussed in the Introduction. Due to interface cooling during droplet evaporation, the surface temperature may change along the droplet surface, and so does the surface (saturated) vapour concentration. Therefore, the surface vapour concentration can become a function of the droplet surface coordinates, which is α in the toroidal coordinate system, and we have

$$C(\alpha, 3\pi-\theta) = C_s(\alpha) \quad [4]$$

where $C_s(\alpha)$ is the surface vapour concentration which is a function of α. Inserting [4] into Eq. [3] gives

$$\int_0^\infty E_\tau P_{i\tau-1/2}(\cosh\alpha)\cosh\left[\tau(\pi-\theta)\right]d\tau = \frac{C_s(\alpha)}{\sqrt{2\cosh\alpha+2\cos\theta}} \quad [5]$$

where $C_s = (C_s - C_\infty)/(C_e - C_\infty)$ is the normalised saturated vapour concentration.

Integral Eq. [5] must be solved for E_τ. The Mehler-Fock integral transform (Magnus et al., 1966) can be used to solve the integral equation and gives

$$E_\tau = \frac{\cosh\tau\theta}{\cosh\tau\pi\cosh\left[\tau(\pi-\theta)\right]} + \frac{\tau\tanh\tau\pi}{\cosh\left[\tau(\pi-\theta)\right]}\int_0^\infty \frac{P_{i\tau-1/2}(\cosh x)\sinh x}{\sqrt{2\cosh x+2\cos\theta}}\left[C_s(x)-1\right]dx \quad [6]$$

In establishing the solution for E_τ as a function of the integration dummy, τ, we used the following integral: (Gradshteyn and Ryzhik, 2007) $(2\cosh\alpha+2\cos\theta)^{-1/2} = \int_0^\infty \cosh(\tau\theta)\,\mathrm{sech}(\tau\pi)\,P_{i\tau-1/2}(\cosh\alpha)\,d\tau$.

Knowing the vapour density, the net of the surface diffusive flux, J, can be determined by Fick's first law, yielding: $J(\alpha) = (D/R)(\cosh\alpha+\cos\theta)(\partial C/\partial\beta)_{\beta=3\pi-\theta}$ (Nguyen et al., 2012). Employing Eqs. [6] and [3] we obtain, after some algebra,

$$J(\alpha) = \frac{(C_e-C_\infty)}{R/D}\left\{C_s(\alpha)\frac{\sin\theta}{2} + \sqrt{2}(\cosh\alpha+\cos\theta)^{3/2}\times \int_0^\infty P_{i\tau-1/2}(\cosh\alpha)\frac{\tau\cosh\tau\theta\tanh\left[\tau(\pi-\theta)\right]d\tau}{\cosh\tau\pi} + (\cosh\alpha+\cos\theta)^{3/2}\,I(\theta)\right\} \quad [7]$$

where $I(\theta) = \int_0^\infty \tau\sinh\left[\tau(\pi-\theta)\right]P_{i\tau-1/2}(\cosh\alpha)G(\tau,\theta)\,d\tau$, and $G(\tau,\theta)$ describes the second term on the right-hand side of Eq. [6], i.e.,

$$G(\tau,\theta) = \frac{\tau\tanh\tau\pi}{\cosh\left[\tau(\pi-\theta)\right]}\int_0^\infty \frac{P_{i\tau-1/2}(\cosh x)\sinh x}{\sqrt{2\cosh x+2\cos\theta}}\left[C_s(x)-1\right]dx \quad [8]$$

Equations [3], [6] and [7] present the new models for the sessile droplet evaporation with varying vapour density along the droplet surface.

3. Results and Discussion

If the vapour density at the droplet surface is constant, we have $C_s(x) = C_e$ for all *x*, and the integrand of the second term of Eq. [6] is equal to zero. Hence, $G(\tau, \theta) = 0$ and $I = 0$. Under these conditions, Eq. [3] reduces to the known prediction(Nguyen et al., 2012), and Eq. [7] for the vapour surface flux reduces to the classical model described by Eq. [1].

It is also noted that our analytical solution described by Eq. [7] is not subject to any restrictions on contact angle θ, such as thin drops (Dunn et al., 2008; Saxton et al., 2016), nor mathematical approximations of numerical results (Picknett and Bexon, 1977; Semenov et al., 2014). Hence, it is generally valid for all contact angles (0 to 180 degrees). It is also valid if the assumption about the spherical cap remains valid and the complex mapping of the droplet surface by the toroidal coordinates is applicable. If this condition is not met, then the whole theory has to be revised by numerical computation – no analytical solutions are available for evaporation of non-spherical drops (except for the thin drop approximations).

Comparing with the recent model described by Eq. [2], the new prediction given by Eq. [7] developed in this paper contains one more term (as described by the integral *I*), which arises from the change in the vapour density at the droplet surface. Upon expanding, the first term of the new prediction for the surface flux is identical to the first term of the recent model described by Eq. [2]. The other remaining terms of the two model equations are different because of the changing vapour surface density. These differences highlight how predictions for evaporation with interface cooling, cannot be developed by simply replacing the interface density in the classical models with the varying vapour density at the droplet surface.

The saturated vapour density on the droplet surface is needed for calculating the surface flux as described by Eq. [7]. Typical experimental results for water droplets are shown in Figure 2. The density is determined using available literature data for the water droplet surface temperature and the empirical correlations given in the Supplementary Material. Figure 2 shows a significant decrease in the saturated vapour density along the droplet surface by interface cooling. In the cases of contact angles θ = 160^o and 110^o, although the ambient temperature and humidity of the surrounding were maintained at about 20.5 - 21 ^{o}C and 29 ± 1%, respectively (Briones et al., 2012; Gleason and Putnam, 2014), the decrease in the vapour density could not be neglected. In the case of θ = 78.5^o, the temperature of the solid planar surface was close to the boiling temperature of

water and, hence, the variation of the vapour density along the droplet surface was as rapid and extensive as shown in Figure 2.

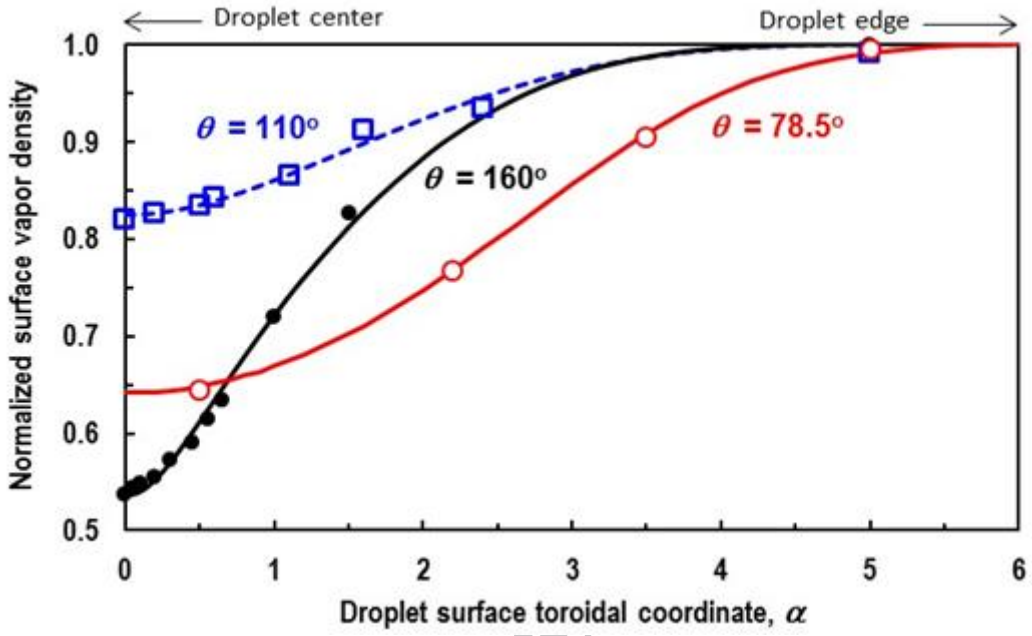

Figure 2. Results for saturated vapour density, $C_s(\alpha)=(C_s-C_\infty)/(C_e-C_\infty)$, at the water droplet surface as calculated using the literature data (Gleason and Putnam, 2014) and the empirical correlations for C_s vs. T as shown in Supporting Material (points), and the best fit of Eq. [9] (lines).

For carrying out the integrals in Eq. [7], a continuous dependence of the vapour density on the droplet surface coordinate, $\alpha \in \langle 0,\infty)$, is needed. Therefore, a number of empirical correlations for describing the available results (Figure 2) were developed asymptotically. It was found that the results can be described by the following empirical equation for C_s vs. α:

$$C_s(\alpha)=1-B\exp\left[-p\sqrt{2\cosh\alpha+2\cos\theta}\right] \qquad [9]$$

where B and p are the model parameters. They can be obtained by the best fit with the experimental results. The fitting with the results shown in Figure 2 give B = 0.588 and p = 0.679 for θ = 160°; B = 0.333 and p = 0.558 for θ = 110°; and B = 0.597 and p = 0.313 for θ = 78.5°. The vapour density at the droplet edge as calculated from the measured temperature is C_e = 17.755, 17.775 and 595.235 g/m^3 for θ = 160°, 110° and 78.5°, respectively. The alternative correlation is $C_s(\alpha)=1-B\exp\left[-p(\cosh\alpha+\cos\theta)^n\right]$, where the model parameters B, n and p can be

determined by the best fit. These correlations can be used to perform the required numerical integration. However, Eq. [9] is mathematically tractable because it can be used to carry out the needed integrations analytically. The analytical results of integration are also advantageous because they remove at least one long step of the numerical calculation of I_1 in Eq. [7]. This double integral involves highly oscillatory and slowly decaying special functions over an infinite range.

If the approximation described by Eq. [9] is used, E_τ in Eq. [6] and the integral of the third term I in Eq. [7] can be simplified to

$$E_\tau = \frac{\cosh \tau\theta}{\cosh \tau\pi \cosh\left[\tau\left(\pi-\theta\right)\right]}\left[1-B\frac{2\tau \sinh \tau\pi}{\pi \cosh \tau\theta} K_{i\tau}\left(p\exp\frac{i\theta}{2}\right)K_{i\tau}\left(p\exp\frac{-i\theta}{2}\right)\right] \quad [10]$$

$$I = -B\frac{2}{\pi}\int_0^\infty \tau^2 \tanh \pi\tau \tanh\left[\left(\pi-\theta\right)\tau\right] P_{i\tau-1/2}\left(\cosh\alpha\right) K_{i\tau}\left(p\exp\frac{i\theta}{2}\right)K_{i\tau}\left(p\exp\frac{-i\theta}{2}\right)d\tau \quad [11]$$

where *K* describes the Bessel function of the second kind. A special feature of Eqs. [10] and [11] is that they can account for the interfacial cooling effect via the model parameter *B*, but if *B* = 0, our general solution presented in this paper can recover the classical theory as discussed below. Therefore, our theory as presented by Eqs. [7], [10] and [11] is generally valid and does not subject to any restrictions or special conditions of use.

When the effect of evaporative cooling is neglected, i.e. $B=0$ in Eqs. [9] and [10], the present model reduces to the classical model as follows:

$$C_{classic}\left(\alpha,\beta\right) = \sqrt{2\cosh\alpha - 2\cos\beta}\int_0^\infty P_{i\tau-1/2}\left(\cosh\alpha\right)\frac{\cosh\theta\tau\cosh\left[\left(2\pi-\beta\right)\tau\right]}{\cosh\pi\tau\cosh\left[\left(\pi-\theta\right)\tau\right]}d\tau \quad [12]$$

From this equation, the classical evaporative flux in Eq. [1] is obtained. Now Eq. [7] can easily be numerically integrated to calculate the evaporative flux along the droplet surface. The numerical integration was efficiently carried out using the Wolfram Mathematica software (Version 10.1). The contour plots for the vapour concentration in the gas phase (Figure 3) show a significant difference in the distribution of vapour concentration between the classical and new models.

The calculation of the toroidal function was calculated using the Mathematica function "LegendreP". The classical model, Eq. [1], predicts that the normalized evaporative flux is a sum of two terms $J_{classic} = J_1 + J_2$, while $J_{GP} = C_s\left(J_1 + J_2\right)$ from the Gleason-Putnam model (Eq. [2]). The semi-analytical model developed in this paper, on the other hand, predicts a sum of three terms in the evaporative flux equation, i.e. $J_{corrected} = C_s J_1 + J_2 + J_3$. In these equations, J_1 and J_2 are the

first and the second term in Eq. [1], respectively, and J_3 is the third term associated with I in Eq. [7]. Since $C_s \leq 1$ and is an increasing function of α, J_{GP} is smaller than $J_{classic}$ but their difference will gradually decrease towards the droplet's edge. Figure 3 shows the comparison of the three models for the evaporative flux for the acute ($\theta = 78.5^o$) and obtuse ($\theta = 160^o$) contact angle cases. The variation of the flux versus the radial coordinate for the other obtuse contact angle ($\theta = 110^o$) case is similar to that of the $\theta = 160^o$ case. Therefore, it is not shown in Figure 4.

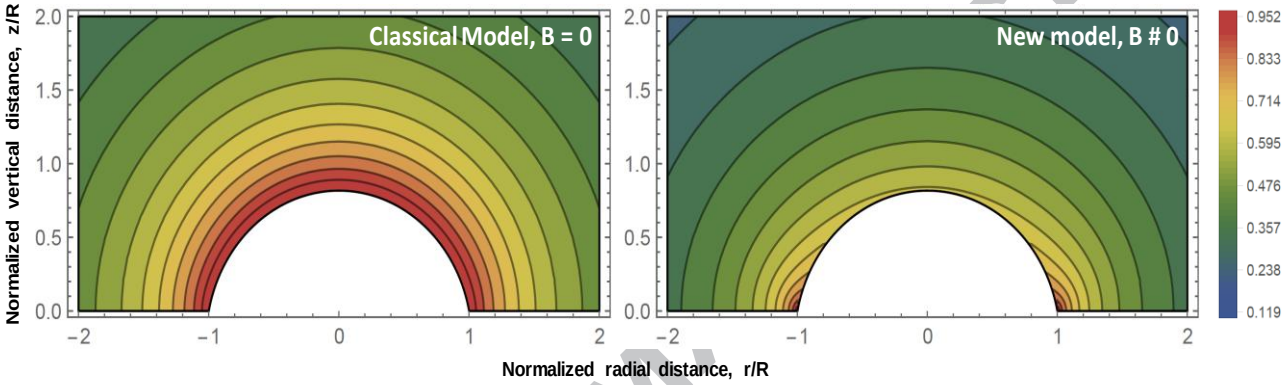

Figure 3. Contour plot of vapour distribution above a sessile droplet ($\theta = 78.5^o$) using the classical model and the new model developed in this paper, as described by Eqs. [3] and [10] with $B = 0$ and $B = 0.597$, respectively. Towards the droplet centre, the interfacial cooling effect leads to a gradual decrease of temperature along the air-liquid interface; thus, a significant lower saturated vapour concentration near the droplet centre is predicted in comparison with the classical model. The colour bar represents the normalized vapour concentration, $(C_s - C_\infty)/(C_e - C_\infty)$.

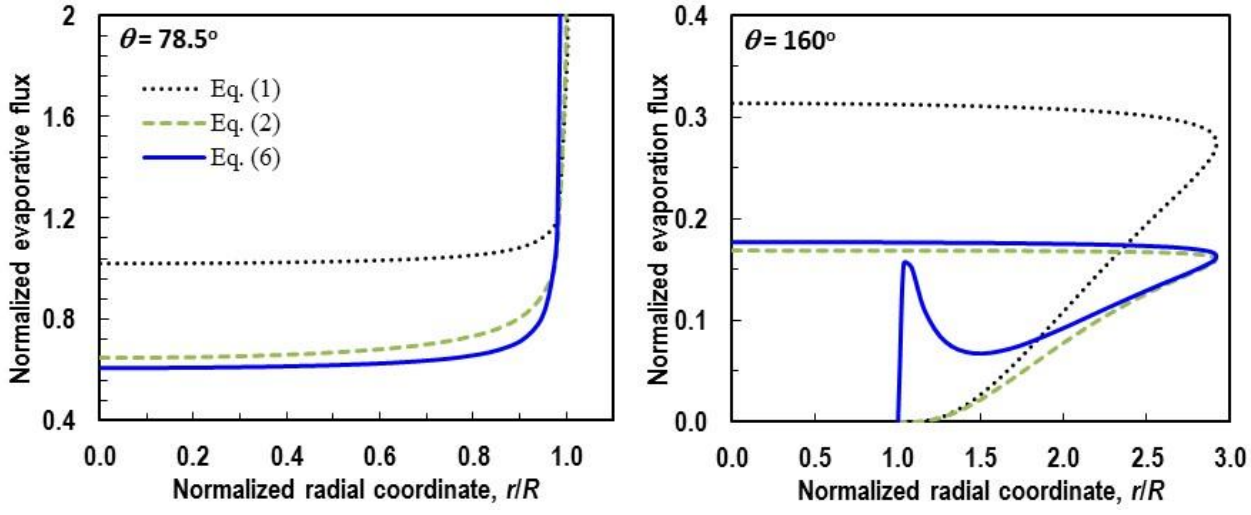

Figure 4. Comparison of three models for normalized evaporative flux $J = J/\left[D\left(C_e - C_\infty\right)/R\right]$ versus normalized radial position r/R. The legends also show the contact angle between the droplet and the substrate.

As can be seen from Figure 4, in the case of an acute contact angle, all three models show that the flux increases from the droplet surface centre (r = 0) to the droplet edge (r = R), where the flux goes to infinity. As previously commented (Poulard et al., 2005), the singularity of the evaporative flux is due to the difference between molecules diffusing away from and back to the liquid phase per unit time. At the edge of the droplet with an acute contact angle, the probability of molecules diffusing back to the droplet interface decreases and, consequently, the evaporative flux by diffusion increases towards the droplet edge. Nonetheless, of the three models, the classical model with constant vapour density as described by Eq. [1] predicts the highest local flux for $r < R$. Likewise, the new model described by Eq. [7] gives the lowest prediction for the local surface flux for $r < R$. However, in the proximity of the droplet edge ($r \rightarrow R$), the new model described by Eq. [7] predicts more rapid increase in the local surface flux than the other two models.

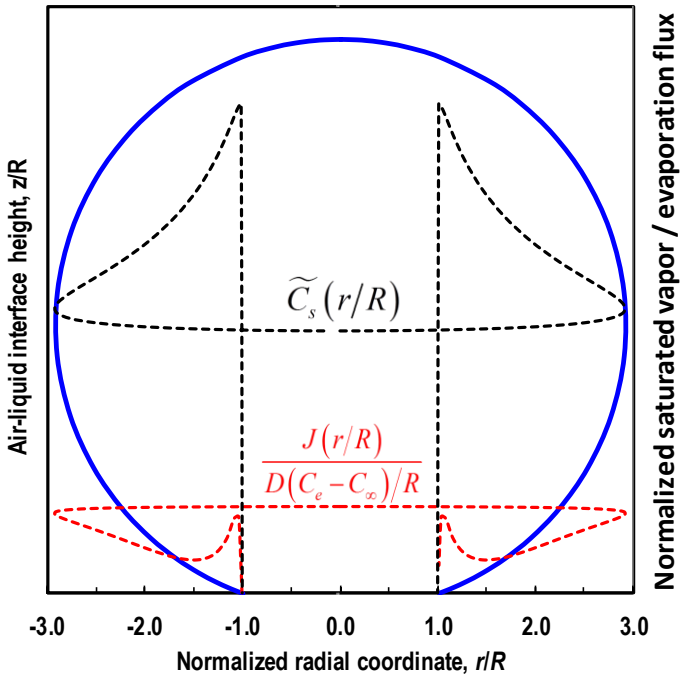

Figure 5. Changes in the evaporative flux in according to the changes in saturated vapour concentration along the air-liquid interface of a sessile droplet $\theta = 160^{o}$.

In the case of an obtuse contact angle, all three models predict that the flux asymptotically approaches zero at the droplet edge ($r = R$) as shown in the right panel of Figure 4. Particularly, of these three models, only the new model described by Eq. [7] shows a rapid increase in the surface flux in the proximity of the droplet edge ($r \rightarrow R$), reaching a maximum and then a minimum before increasing to the maximum at the droplet surface centre. Evidently, this significant change in the local flux at the droplet surface as predicted by the new model is due to the modified first term and the third (new) term (i.e., the integral I) on the right-hand side of Eq. [7]. The strong evaporative cooling at the droplet apex means that the contact line region has the highest local temperature, thus inducing the highest local saturated vapour concentration (Figures 4 and 5). This greatest spatial vapour gradient can be the reason of rapidly increasing evaporative fluxes predicted at the proximity of the contact line. Our model is also in agreement with previous numerical results reported for a water droplet with a contact angle of 170° (Pan et al., 2014). It is worth noting that this behaviour happens for droplets of both acute and obtuse contact angles, however, it stands out for the latter case since the classical flux is decreasing towards the contact line.

4. Conclusion

In this paper, the process of diffusion-driven evaporation of sessile droplets on a solid planar surface has been re-considered and modelled by taking into account the interface cooling which changes the saturated vapour density at the droplet surface. The corresponding process of evaporation was mathematically re-modelled by applying the physically consistent boundary condition for saturated vapour density at the droplet surface. The new model obtained for the local evaporative flux reduces to the classical models if the saturated vapour density is constant along the droplet surface. If the vapour density is not constant, the new models can be significantly different from the models available in the literature, especially in the case of droplets with obtuse contact angle. The experimental results for the temperature of the droplet surface available in the literature were converted to the saturated vapour density (and empirically correlated with the surface coordinate) which was valuable for the demonstration of the models. The new model equations present the key corrections to the predictions of the spatial distribution of vapour density around the droplet and surface diffusive flux. The presented analysis shows a significant effect of interface cooling at the droplet surface which should be considered in predicting diffusion-driven evaporation of sessile droplets.

Acknowledgments

This research was supported under Australian Research Council's Linkage Projects funding scheme (project number LP0989217).

References

Briones, A.M. et al. (2012). Evaporation Characteristics of Pinned Water Microdroplets. *J. Thermophys. Heat Transfer*, 26: 480−493.

Deegan, R.D. et al. (1997). Capillary flow as the cause of ring stains from dried liquid drops. *Nature*, 389(6653): 827-829.

Dunn, G.J., Wilson, S.K., Duffy, B.R., David, S. and Sefiane, K. (2008). A mathematical model for the evaporation of a thin sessile liquid droplet: Comparison between experiment and theory. *Colloids and Surfaces A*, 323(1-3): 50-55.

Erbil, H.Y. (2015). Control of stain geometry by drop evaporation of surfactant containing dispersions. *Adv. Colloid Inter. Sci.*, 222: 275-290.

Gleason, K. and Putnam, S.A. (2014). Microdroplet evaporation with a forced pinned contact line. *Langmuir*, 30(34): 10548–10555.

Gradshteyn, I.S. and Ryzhik, I.M. (2007). *Table of integrals, series and products*. Elsevier, Amsterdam, 1171 pp.

Hu, H. and Larson, R.G. (2002). Evaporation of a sessile droplet on a substrate. *J. Phys. Chem. B*, 106(6): 1334-1344.

Magnus, W., Oberhettinger, F. and Soni, R.P. (1966). *Formulas and Theorem for Special Functions of Mathematical Physics*. Springer-Verlag, New York, 476 pp.

Nguyen, T.A.H. and Nguyen, A.V. (2012a). Increased evaporation kinetics of sessile droplets by using nanoparticles. *Langmuir*, 28(49): 16725-16728.

Nguyen, T.A.H. and Nguyen, A.V. (2012b). On the Lifetime of Evaporating Sessile Droplets. *Langmuir*, 28(3): 1924-1930.

Nguyen, T.A.H. et al. (2012). Theoretical and experimental analysis of droplet evaporation on solid surfaces. *Chem. Eng. Sci.*, 69(1): 522-529.

Pan, Z.H., Weibel, J.A. and Garimella, S.V. (2014). Influence of Surface Wettability on Transport Mechanisms Governing Water Droplet Evaporation. *Langmuir*, 30(32): 9726-9730.

Picknett, R.G. and Bexon, R. (1977). The evaporation of sessile or pendant drops in still air. *J. Colloid Interface Sci.*, 61(2): 336-350.

Popov, Y.O. (2005). Evaporative deposition patterns: spatial dimensions of the deposit. *Phys. Rev. E*, 71(3): 036313.

Poulard, C., Guena, G. and Cazabat, A.M. (2005). Diffusion-driven evaporation of sessile drops. *J. Phys. Condensed Matter*(49): S4213.

Saxton, M.A., Whiteley, J.P., Vella, D. and Oliver, J.M. (2016). On thin evaporating drops: When is the d2-law valid? *J. Fluid Mech.*, 792: 134-167.

Semenov, S. et al. (2014). Simultaneous spreading and evaporation: recent developments. *Adv. Colloid Inter. Sci.*, 206: 382-398.

Highlights

- Evaporation changes temperature and vapour density at sessile droplet interfaces.
- New predictions for interface vapour density and evaporative flux are obtained.
- New predictions reduce to classical models if interface cooling is negligible.
- Comparison with the literature data shows significant effects of interface cooling.

GRAPHICAL ABSTRACT